Highlights from the Large High-Altitude Air-Shower Observatory (LHAASO)

Domenico della Volpe^{a,*} **and LHAASO Coll.**

^{a}*Université de Genevè,*
Quai Ernest-Ansermet 24 , 1205 Genevè , Switzerland

E-mail: domenico.dellavolpe@unige.ch

The Large High-Altitude Air Shower Observatory (LHAASO) opened the multi-TeV era in γ-astronomy and cosmic ray physics. Since July 2021, LHAASO is fully operational and collecting high-quality data. A Nature paper in 2021, revealing 12 VHE new sources, was just the start of LHAASO science, revealing the huge scientific potential of LHAASO. Many analysis efforts are ongoing in different areas and several results are already published. In this contribution, we will show some highlights from LHAASO science in particular on the Crab SED at PeV energies, the new limits on the Lorentz Invariance Violation and Dark Matter.

---

*Speaker

1.   The LHAASO Observatory

LHAASO is a new generation multi-purpose experiment. A detailed description of the system and the its physics goals can be found in the LHAASO Science book [1]. Here we will briefly describe the system for a correct understanding of the results discussed later.

Figure 1: A bird-eye picture of LHAASO. The 3 central ponds of WCDA are clearly visible in the center, while the K2MA array is the area within the yellow ring.

LHAASO has been built at 4410 m a.s.l. on top of the Haizi mountain in the Sichuan region of China. Fig 1 shows a bird-eye view of the LHAASO installation, which covers an area of 1.3 km in diameter.

In the middle of the array, it is sitting the large Water Cherenkov Detector Array (WCDA) complex, composed of three ponds covering an area of 78'000 m^2 (see Fig. 1). The WCDA is segmented into 3120 square cells, with a side of 5 m separated by a black curtain to impede light cross-talk. The water level in the cell is 4.4 m above the ground. In each cell, 2 PMT of different sizes are installed to accommodate a very large photon dynamic range. While in the WCDA-1 are installed 8" and 1.5" PMTs, in the other two ponds are installed 20" and 3" PMT in order to lower the energy threshold below the 100 GeV of the original design.

The km-square array (KM2A), surrounding the WCDA complex, is composed of 1171 Muon detectors (MD), arranged on a triangular grid with a spacing of 30 m, and 5195 electromagnetic detectors (ED) arranged on a triangular grid with a spacing of 15 m. The MD is a tank of 6 m in diameter with a height of 1.5 m buried under 2.5 m of dirt to shield it from muon with energy less than 1 GeV. In the center of the tank, facing up under 1.2 m of water, a single PMT is installed.

The ED is a scintillator plane of 1 m^2 to detect the electromagnetic component of the cascade. It is composed of four tiles wrapped with a layer of Tyvek to improve photon collection efficiency and readout by a single PMT. A 5 mm thick layer of lead is added on top to absorb low energy charged particles and convert γ into electron-positron pairs in order to increase detection efficiency.

The installation is completed with the Wide Field of View Cherenkov telescope array (WCFTA), consisting of 18 telescopes with a field of view of $16° \times 16°$ and with a pixel size of approximately $0.5° \times 0.5°$.

The telescopes are realized inside a standard container to protect its elements from the harsh condition of the site. A 5 m^2 segmented spherical mirror is installed at the back of the container, while in the front part a camera is installed. The camera features an array of 32×32 pixels, each realized by a SiPM coupled to a light funnel. A window coated with a cut-off filter to enhance the SNR by cutting the Nigh Sky Background seals the camera and protects the optical elements from the harsh environment.
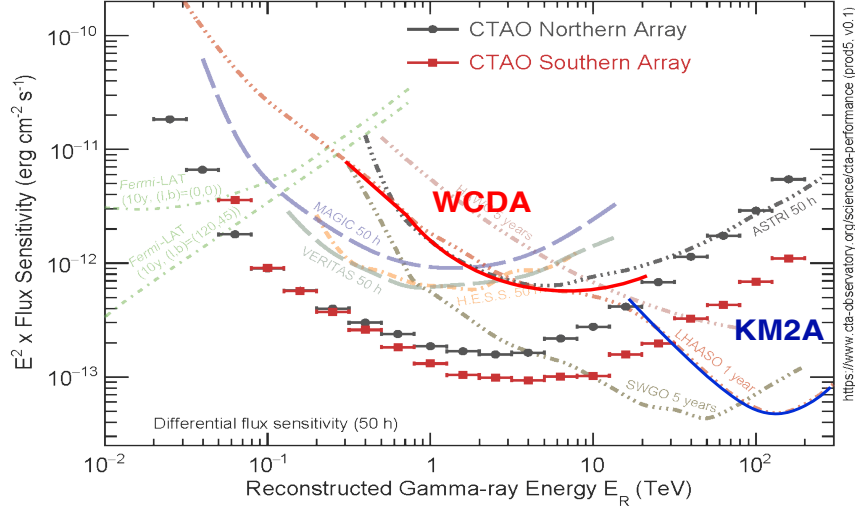

Figure 2: Sensitivity curve oh LHAASO overlaid with current and future instruments.

In Fig. 2, LHAASO sensitivity is shown compared with current and future instruments like CTA or SWGO. LHAASO sensitivity is dominated at low energy (few GeV to 10 TeV) by the WCDA, which is tuned for γ-ray astronomy and extragalactic physics, while KM2A dominates the high energy range. It is also evident how LHAASO will be the most sensitive instrument above 50 TeV for the next decades.

A detailed overview of the Physics potential of LHAASO can be found in the special issue of the Chinese Physics released in 2021 where all science topics are discussed, as Galactic [2] and Extragalactic Physics [3], Cosmic rays Physics [4], Dark Matter and BSM Physics [5], Multi-messenger astronomy [6], and Solar and Heliosphere Physics [7].

Most of the results that will be discussed here have been obtained with the data of the partial array, which started science operation already in 2019 before the completion of the full array in 2021.

2. The new γ-ray sources

In a Nature paper published in 2021 [8], a first survey of the sky with LHAASO has been published, where twelve new sources have been studied and the most energetic ones showed a SED that extends in the multi-TeV range without any sign of cut-off.

Recently, three more sources have been studied in more detail. LHAASO J0341+5258[9] is an extended source with no clear counterpart in other wavelengths and without an energetic pulsar or

young SNRs in the vicinity, a scenario that challenges both the leptonic and hadronic scenarios of gamma-ray production.

LHAASO J2108+5157[10] is a high-energy source that reaches 440 TeV and which has in the neighboring a Giant Molecular cloud suggesting a hadronic production, but the SED cannot yet rule out the leptonic scenario. No obvious counterparts have been found, and deeper multi-wavelength observations will help to cast new light on this intriguing UHE source.
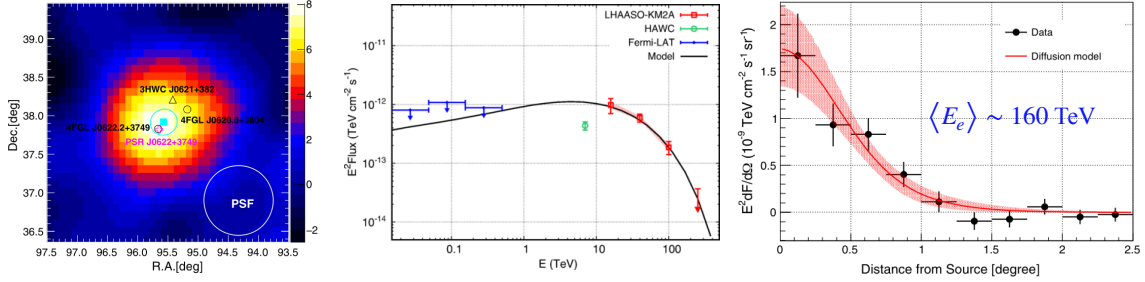

Figure 3: The new source near PSR J0622+3749 extensions (left), SED (center), Diffusion coefficient (right).

Another very high-energy gamma-ray source is around the location of the middle-aged pulsar, PSR J0622+3749 [11]. It is an extended source of about 0.40° with a significance of 4.1 σ (see Fig. 3-left). This source seems to belong to the class of pulsar halos consistent with the slow diffusion of particles in the turbulent medium around pulsars. Also, the diffusion coefficient, assuming a mean energy of the electronic population of 160 TeV, (see Fig. 3-right) is consistent with what is inferred from the HAWC observations of Geminga and Monogem [12].

3. The Crab nebula at PeV energies

The Crab Nebula, the standard candle for γ-ray astronomy is being used also in LHAASO for validating the performance both of WCDA [13] and KM2A [14]. These studies have led for the first time to an extension of the Crab SED up to the PeV [15], which has triggered a lot of interest as it shows some inconsistency with the pure leptonic model of the Crab emission.

Possible interpretations of SED are discussed in a recent work [16], which investigates the multi-band non-thermal radiation with the leptonic and leptonic–hadronic hybrid models. The modeling results indicate that the pure leptonic origin model is compatible with data only in a limited part of the energy range. As a matter of fact, as can be seen in Fig. 4-left, even if the one-zone leptonic model seems to agree quite well with the data, for COMPTEL data there is a disagreement of the order of four σs, which become more than ten for FERMI data.

For this, it is also explored the possibility of a hadronic scenario for the VHE γ-ray. The iron nuclei can escape from the polar car surface of the pulsar and, moving along the magnetic field, reach the pulsar magnetosphere where they can be accelerated by the potential present. After the acceleration of the pulsar magnetosphere, the particles can escape from the pulsar magnetosphere along the open magnetic field lines and be injected into the PWN. During the propagation process, the iron nuclei and the other heavy nuclei will undergo interaction with the background soft photons produced inside the pulsar outer gap and disintegrate. The protons, either directly emitted in the

disintegration process or produced by neutron decay from the evolution process, are captured by the nebula and accumulated in the PWNe.

This further contribution is modeled and fitted to the data, only for energy above 1 GeV, as shown in Fig.4-right. The fit reproduces quite well the data but still at PeV energies it cannot reproduce the correct flux. In the paper, an extra component of the proton spectrum is added, as an exponential cutoff power-law distribution $\frac{dN}{dE} = A_p E_p^{-\alpha_p} \exp\left[\frac{E}{E_{c_p}}\right]$, where the normalization factor A_p is fitted with the PeV region data, while the value for $\alpha_p = 2.0$ and $E_{c_p} = 30$ TeV are chosen from the literature.

It seems that the contribution of hadronic interaction is hardly constrained at the highest energy, where they seem to contribute especially in the energy range exceeding the PeV. More statistics will clearly clarify the picture and LHAASO expect about 1-2 PeV γ-ray per year.

At the same time, the whole picture cannot exclude yet leptonic production, and further data above 100 TeV are needed. Once again is confirmed that the multi-TeV window opened by LHAASO will bring new insight into CR nature.
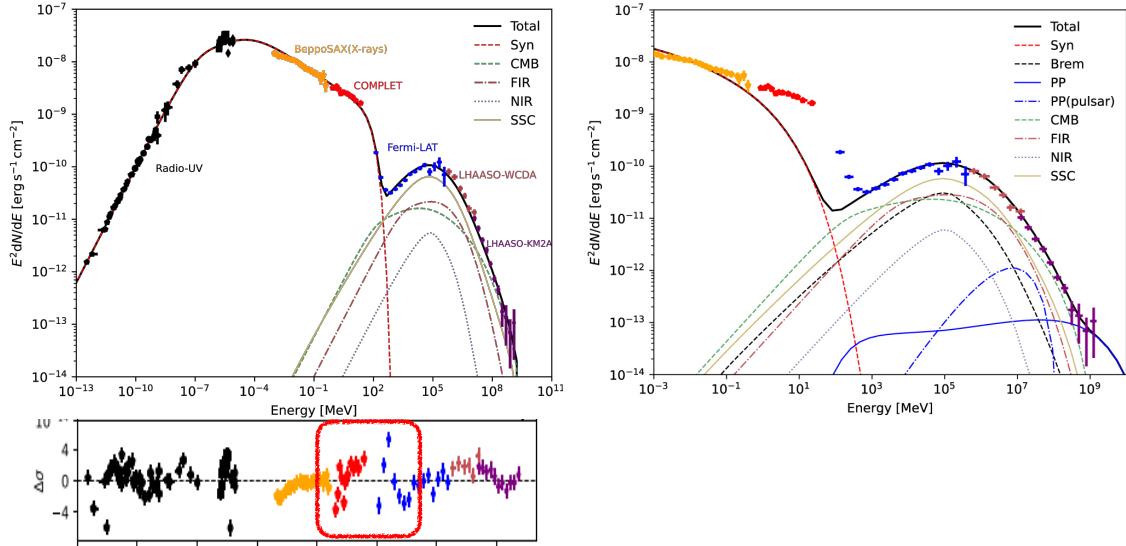

Figure 4: Multi-wavelenght Spectral Energy Density of the Crab nebula, from radio to PeV. A fit for of pure leptonic model on the left. At the bottom of the figure discrepancy up to 4 *sigma* are visible in the non-thermal emission already at FERMI energies. On the right, a fit to the non-thermal data, only, with a leptonic+hadronic production model. This explains the disagreement at lower energies.

4. Lorentz invariant Violation

LHAASO measured the most energetic γ-ray from Crab at 1.1 PeV [15] and also the highest-ever-recorded energy photon, reaching 1.4 PeV from the Cygnus region. These events provide a very sensitive probe of possible Lorentz invariance violation (LIV). At low energies, the LIV interaction can be expressed as an effective model by introducing LIV terms in the SM Lagrangian. These LIV terms will modify the particle dispersion relation, $E_\gamma^2 - p_\gamma^2 = \pm|\alpha_n|p_\gamma^{n+2}$, altering the standard on-shell condition of a particle energy-momentum relation in special relativity. The LIV energy
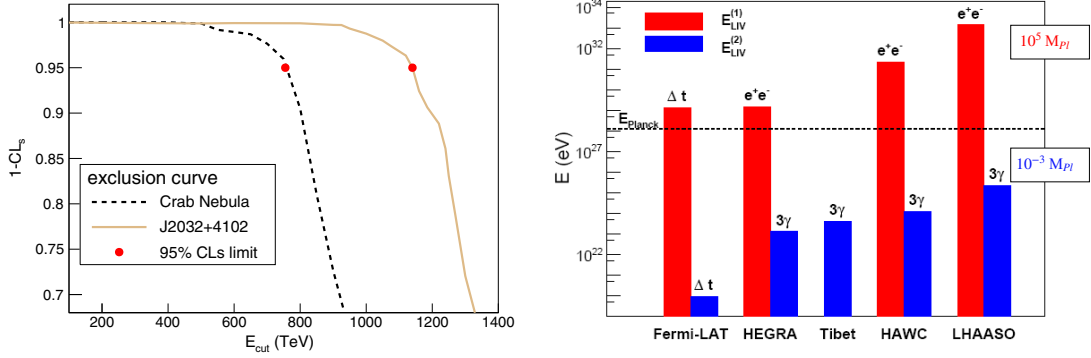
Figure 5: LHAASO limits on LIV for first order from $\gamma \to e^+e^-$ decays, and second order from splitting $\gamma \to 3\gamma$

scale of the nth order is $E_{LIV}^n = \alpha_n^{-1/n}$. In this work, the superluminal case is analyzed (positive α_n) in which the γ can decay in a $e^\pm$ pair, or can split in several photons. The dominant splitting process is $\gamma \to 3\gamma$.

In the superluminal scenario, the decay or splitting of high-energy γ-ray results in a sharp cutoff of the energy spectrum (see Fig. 5-left). Even if no signature of the LIV is found in their energy spectra, it was possible to derive lower limits on the LIV energy scale [17]. The LHAASO limits improve by at least one order of magnitude the previous results [18, 19] (see Fig. 5-right). LHAASO results show that the first-order LIV energy scale should be higher than about 10^5 M_{Planck}, while the second-order LIV scale is greater than 10^{-3} M_{Planck}.

5. Dark Matter

At the time of writing, an update of the Dark matter limits presented at this conference has been accepted on Physics Review Letter [20]. For this, instead of the one presented at the conference, we report here the latest result obtained analyzing 570 days of data with partial array (340 days with 1/2 KM2A array and 230 with 3/4 of the KM2A array).

In the PeV energy range, the dominant γ-ray components are the prompt component generated directly from Galactic DM decays and the secondary component from Inverse Compton (IC) scattering of $e^\pm$ produced by DM particle. For both components, it has been used the Navarro-Frenk-White (NFW) DM halo profile distribution.

The search was conducted in a Region-of-Interest (ROI$_0$), around $15° \leq b \leq 45°$ and $30° \leq l \leq 60°$ in order to be at small galactocentric radius, where DM is expected to be higher, but avoid the diffuse astrophysical emission from Fermi Bubbles and galactic plane. Four other control regions (ROI$_{1...4}$) are used, with the same declination and angular size, to ensure the same detector response to avoid potential systematic related to this. The detector responses of the ROIs is evaluated by tracking the ROIs across the sky and comparing it with detector simulations

The search for a DM signal is done by scanning through the DM mass from 10^5 to 10^9 GeV for each decay channel, assuming a 100% branching fraction. No significant detection of DM signals is found but the one-sided 95% lower limit on the DM decay lifetime, τ_{DM} has been calculated. The limits, shown in Fig. 6 for both $b\bar{b}$ (left) and $\tau\bar{\tau}$ (right) decay, have been derived for each DM mass and decay channel by minimizing the Likelihood for both τ_{DM} and background model. It is
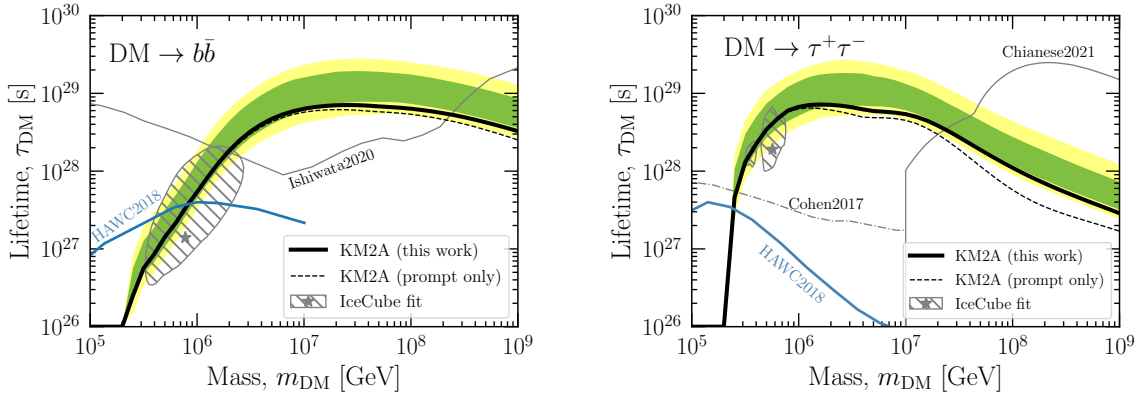
Figure 6: One-sided lower limits at 95% on DM lifetime obtained for DM decaying into b quarks (left) or τ leptons (right). The black dashed line shows the limit obtained considering prompt DM contribution only. The green (68%) and yellow bands (95%) correspond to background-only hypothesis expected from Monte Carlo simulations. Previous limits [21–23] and those from HAWC [11] are shown with gray and blue lines. The hatched regions show the 1-σ DM parameter space favored by IceCube high-energy neutrino flux [24].

worth mentioning that around 10 PeV a significant improvement is visible in Fig. 6 for both the $b\bar{b}$ decay channel, where almost a factor 5 is achieved, and $\tau\bar{\tau}$ where the factor is almost 10. This confirms LHAASO as the best instrument in these searches in the PeV energy region.

6. Acknowledgements

References

[1] LHAASO Collaboration 2022 *Chinese Physics C* **46** 030001 URL https://doi.org/10.1088/1674-1137/ac3fa6

[2] LHAASO Collaboration 2022 *Chinese Physics C* **46** 030002 URL https://doi.org/10.1088/1674-1137/ac3fa8

[3] LHAASO Collaboration 2022 *Chinese Physics C* **46** 030003 URL https://doi.org/10.1088/1674-1137/ac3fa9

[4] LHAASO Collaboration 2022 *Chinese Physics C* **46** 030004 URL https://doi.org/10.1088/1674-1137/ac3faa

[5] LHAASO Collaboration 2022 *Chinese Physics C* **46** 030005 URL https://doi.org/10.1088/1674-1137/ac3fab

[6] LHAASO Collaboration 2022 *Chinese Physics C* **46** 030006 URL https://doi.org/10.1088/1674-1137/ac3fac

[7] LHAASO Collaboration 2022 *Chinese Physics C* **46** 030007 URL https://doi.org/10.1088/1674-1137/ac3fae

[8] LHAASO Coll 2021 *Nature* **594** 33–36 ISSN 1476-4687 URL https://doi.org/10.1038/s41586-021-03498-z

[9] LHAASO Coll 2021 *The Astrophysical Journal Letters* **917** L4 URL https://doi.org/10.3847/2041-8213/ac0fd5

[10] LHAASO Coll 2021 *The Astrophysical Journal Letters* **919** L22 URL https://doi.org/10.3847/2041-8213/ac2579

[11] LHAASO Coll (LHAASO Collaboration) 2021 *Phys. Rev. Lett.* **126**(24) 241103 URL https://link.aps.org/doi/10.1103/PhysRevLett.126.241103

[12] HAWC Coll 2017 *Science* **358** 911–914 URL https://www.science.org/doi/abs/10.1126/science.aan4880

[13] LHAASO Coll (LHAASO) 2021 *Chin. Phys. C* **45** 085002

[14] LHAASO Coll 2021 *Chinese Physics C* **45** 025002 URL https://doi.org/10.1088/1674-1137/abd01b

[15] LHAASO Coll 2021 *Science* **373** 425–430 (*Preprint* https://www.science.org/doi/pdf/10.1126/science.abg5137) URL https://www.science.org/doi/abs/10.1126/science.abg5137

[16] Nie L, Liu Y, Jiang Z and Geng X 2022 *The Astrophysical Journal* **924** 42 URL https://doi.org/10.3847/1538-4357/ac348d

[17] LHAASO Coll (LHAASO Collaboration) 2022 *Phys. Rev. Lett.* **128**(5) 051102 URL https://link.aps.org/doi/10.1103/PhysRevLett.128.051102

[18] HAWC Coll (HAWC Collaboration) 2020 *Phys. Rev. Lett.* **124**(13) 131101 URL https://link.aps.org/doi/10.1103/PhysRevLett.124.131101

[19] Astapov K, Kirpichnikov D and Satunin P 2019 *Journal of Cosmology and Astroparticle Physics* **2019** 054–054 URL https://doi.org/10.1088/1475-7516/2019/04/054

[20] LHAASO Coll (LHAASO) 2022 *arXiv* **astro-ph.HE** URL https://doi.org/10.48550/arXiv.2210.15989

[21] Cohen T, Murase K, Rodd N L, Safdi B R and Soreq Y 2017 *Phys. Rev. Lett.* **119**(2) 021102 URL https://link.aps.org/doi/10.1103/PhysRevLett.119.021102

[22] Ishiwata K, Macias O, Ando S and Arimoto M 2020 *Journal of Cosmology and Astroparticle Physics* **2020** 003 URL https://dx.doi.org/10.1088/1475-7516/2020/01/003

[23] Chianese M, Fiorillo D F, Hajjar R, Miele G and Saviano N 2021 *Journal of Cosmology and Astroparticle Physics* **2021** 035 URL https://dx.doi.org/10.1088/1475-7516/2021/11/035

[24] Chianese M, Fiorillo D F, Miele G, Morisi S and Pisanti O 2019 *Journal of Cosmology and Astroparticle Physics* **2019** 046 URL https://dx.doi.org/10.1088/1475-7516/2019/11/046

PoS(NOW2022)048